Journal of Applied Polymer Science

Ethylene Vinyl Acetate/Nanoclay-Based Pigment Composites: Morphology, Rheology, and Mechanical, Thermal, and Colorimetric Properties

Veronica Marchante, Veronica Benavente, Antonio Marcilla, Francisco Miguel Martínez-Verdú, Maria Isabel Beltrán

University of Alicante, Carretera San Vicente s/n, 03690, San Vicente del Raspeig, Alicante, Spain

Correspondence to: V. Marchante (E-mail: veronica.marchante@ua.es)

ABSTRACT: In this study, a new type of nanopigment, obtained from a nanoclay (NC) and a dye, was synthesized in the laboratory, and these nanopigments were used to color an ethylene vinyl acetate (EVA) copolymer. Several of these nanoclay-based pigments (NCPs) were obtained through variations in the cation exchange capacity (CEC) percentage of the NC exchanged with the dye and also including an ammonium salt. Composites of EVA and different amounts of the as-synthesized nanopigments were prepared in a melt-intercalation process. Then, the morphological, mechanical, thermal, rheological, and colorimetric properties of the samples were assessed. The EVA/NCP composites developed much better color properties than the samples containing only the dye, especially when both the dye and the ammonium salt were exchanged with NC. Their other properties were similar to those of more conventional EVA/NC composites. © 2013 Wiley Periodicals, Inc. J. Appl. Polym. Sci. 130: 2987–2994, 2013

KEYWORDS: composites; dyes/pigments; nanostructured polymers; optical properties; thermoplastics

Received 6 February 2013; accepted 17 April 2013; Published online 17 June 2013

DOI: 10.1002/app.39422

INTRODUCTION

During the last few decades, polymeric nanocomposites based on organically modified clays have attracted great scientific interest. The mechanical, barrier, and thermal properties of these polymers improve with only small amounts of additives.[1–3] Specifically, ethylene vinyl acetate (EVA) nanocomposites form intercalated and exfoliated structures without the addition of compatibilizers;[4–8] these could be due to the high polarity of the EVA copolymer and its fluidity at high temperatures.[9] The formation of intercalated or exfoliated morphologies depends on the type of nanoclay (NC), the vinyl acetate (VA) content, and the processing conditions.[5] Marini et al.[10] evaluated the influence of the matrix viscosity on the extent of exfoliation of EVA/organoclay nanocomposites. They concluded that the presence of high interactions between the polar surfactant and the matrix groups is extremely important but not enough to guarantee exfoliation and an efficient clay dispersion. The matrix viscosity should be low enough to promote the entrance of polymeric chains inside the clay galleries and high enough to create shear tensions during processing to break and disperse clay tactoids. Jeon et al.[11] investigated the effect of the VA content, the molecular weight of EVA, and the type of surfactant in the clay dispersion. These authors observed that the type of surfactant of the clay played a critical role in the composite behavior. Wilson et al.[12] studied the gas-transport properties of EVA/clay nanocomposite membranes. According to these authors, the dispersion of nanoparticles presented a maximum at a weight content of 3% of NC, and the agglomeration increased at higher clay loadings. Chaudhary et al.[8] studied EVA nanocomposites using matrices with various VA and oganoclay contents and also analyzed the clay–polymer interaction and their influence on the crystallinity of the matrix and the mechanical properties. They found that a high polarity facilitated greater clay platelet dispersion. Furthermore, other authors have studied the rheological properties of nanocomposites to obtain information about their structure. For example, Pasanovic-Zujo et al.[4] studied the shear and extensional properties of exfoliated EVA nanocomposites with different VA contents and different clay loadings. They observed that exfoliated nancomposites exhibited enhanced properties in steady and dynamic flux, whereas intercalated nanocomposites showed only a slight increase compared to the neat polymer. Gupta et al.[13] investigated the structure and morphology of organobentonite on the rheological properties of nanocomposites of an ethylene vinyl acetate with 28% of vinyl acetate (EVA28) using different clay loadings. Although complete exfoliation was not achieved, the EVA28 nanocomposites showed a significant increase in the shear viscosity as well as in the storage and loss moduli. They

also found that the presence of silicate layer networks could have induced solidlike behavior and reduced strain hardening phenomena under a uniaxial extensional flow.

NCs are generally modified with cationic surfactants, such as quaternary ammonium salts (SAs).[14–17] Nevertheless, Fischer and Batenburg[18] modified the NC with organic dye molecules to obtain a novel type of nanopigment. In this study, this kind of organically modified NC was used. This nanoclay-based pigment (NCP) could be applied to a wide variety of substrates to make coatings or to color a material, but other applications have not been developed yet. NCPs are expected to improve some properties while giving color; this would make it possible to reduce the amount of additives used and thereby the cost. In previous studies,[19,20] NCPs were applied to linear low-density polyethylene (PE). It was found that samples with the NCPs developed better color performance and gave a wider color gamut that the samples colored with the conventional dye. In addition, other properties of the PE/NCP samples were improved or not affected.

The main purpose of this study was to assess the effect of the NCPs in EVA. On the basis of our previous experience in the preparation of PE/NCP composites[20] and EVA/NC composites,[21] we expected that the incorporation of NCPs into EVA would result in the formation of composites with improved color properties. To assess the influence of the dye content in the NCPs, several nanopigments with different contents of the dye methylene blue (MB) were used. In a set of samples, NC and MB were used without previous exchange to study the effect of the components of the NCPs. In addition, a novel NCP obtained through the combination of two surfactants simultaneously (MB and an SA) was synthesized and tested in EVA. The morphological, rheological, mechanical, thermal, and optical properties of the EVA mixtures were evaluated.

EXPERIMENTAL

Materials

EVA resin with 18 wt % VA (Escorene Ultra) was supplied by Exxon Mobil Chemical. The NC used was Nanofill 116 provided by Süd-Chemie. Nanofill 116 is a sodium montmorillonite with a cation exchange capacity (CEC) of 120 mequiv/100 g of clay. The NC was organically modified with the organic colorant MB (weight-average molecular weight = 319.85 g/mol) and with an SA, ethyl hexadecyl dimethyl ammonium bromide (weight-average molecular weight = 378.47 g/mol), both supplied by Sigma-Aldrich.

Preparation of the Nanopigments

The synthesis of the NCPs used in this study was described in a previous article.[20] Moreover, in this work, a NCP exchanged with both MB and an SA was also synthesized, where a 20% CEC was performed with MB and an 80% CEC was done with SA. To obtain this nanopigment, once the ionic exchange with the MB was done, a solution containing the required amount of SA was added before filtration.

The synthesized NCPs were named NCP(*X*/*Y*), where *X* is the nominal percentage of CEC exchanged with MB and *Y* is the nominal percentage CEC exchanged with the SA.

Table I. List of Prepared Samples and Their Compositions per 100 g of EVA

Set of samples	Sample	NC (phr)	MB (phr)	SA (phr)
	EVA	—	—	—
EV–NC	EV–NC-0.1	0.1	—	—
	EV–NC-1	1	—	—
	EV–NC-5	5	—	—
EV–MB	EV–MB-0.02	—	0.02	—
	EV–MB-0.07	—	0.07	—
	EV–MB-0.28	—	0.28	—
EV–NC-1–MB	EV–NC-1–MB-0.02	1	0.02	—
	EV–NC-1–MB-0.07	1	0.07	—
	EV–NC-1–MB-0.28	1	0.28	—
EV–NCP(*X*/*Y*)	EV–NCP(5/0)-1	0.98	0.02	—
	EV–NCP(20/0)-1	0.93	0.07	—
	EV–NCP(100/0)-1	0.72	0.28	—
EV–NCP(20/0)	EV–NCP(20/0)-0.1	0.09	0.01	—
	EV–NCP(20/0)-1	0.93	0.07	—
	EV–NCP(20/0)-5	4.65	0.34	—
EV–NCP(20/80)	EV–NCP(20/80)-0.1	0.06	0.01	0.03
	EV–NCP(20/80)-1	0.65	0.07	0.28
	EV–NCP(20/80)-5	3.23	0.34	1.43

Preparation of the EVA Composites

All of the compounds were premixed in a Thermomix Vorwerk 3300 for 2 min at medium speed. The mixtures were blended in a Brabender Plasticorder PL 2000 internal mixer for 10 min at 110°C at a counterrotational blade speed of 15 rpm. Thin films (ca. 1 mm thick) were pressed in a Mecamaq PHF 50 hot-plate press for 10 min at 150°C and 150 bar. The samples were cooled in a plate press refrigerated with water at 10°C for 10 min.

Table I shows all of the prepared samples. In the sample names, EV designates the polymer, NC designates the unmodified nanoclay, MB designates the methylene blue, SA designates the quaternary ammonium salt, and NCP(*X*/*Y*) designates the nanopigment. Separated by a dash, the load of the additives in the samples is indicated in parts per hundred of polymer (phr). There were six sets of samples:

- The EV–NC set corresponded to the EVA samples that contained unmodified NC.
- The EV–MB set corresponded to the EVA samples that contained MB.
- The EV–NC-1–MB set corresponded to the samples that contained 1 phr of NC and different amounts of MB without previous exchange between the components (physical mixture).
- The EV–NCP(*X*/*Y*) set was the group of the samples with 1 phr nanopigments synthesized with different contents of MB.
- The EV–NCP(20/0) and EV–NCP(20/80) sets corresponded to the EVA samples that contained different amounts of the nanopigments NCP(20/0) and NCP(20/80).

Table II. List of Nanopigments Synthesized and the Actual CEC Percentages with MB and SA Obtained by CHNS

Nanopigment	Actual CEC exchanged with MB (%)	Actual CEC exchanged with SA (%)
NCP(5/0)	3.9	—
NCP(20/0)	14.5	—
NCP(100/0)	58.2	—
NCP(20/80)	11.4	72.6

The samples from the EV–MB, EV–NC-1–MB, and EV–NCP(*X*/*Y*) sets had similar contents of MB and NC when they had any.

Sample Characterization

A thorough characterization of the NCPs and EVA/NCP composites was carried out with the following tests and techniques: CHNS elemental analysis, X-ray diffraction (XRD), transmission electronic microscopy (TEM), color performance, bleeding testing, mechanical strength, and thermogravimetric analysis. The equipment and conditions were explained in a previous article.[20] In addition, the rheological and calorimetric behavior of the EVA composites were also assessed in this study, as described later.

The dynamic viscosity was measured with a Bohlin CS rheometer at 160°C with a plate 20 mm of diameter at constant strain of 5% and a frequency ranging from 0 to 20 s^{-1}. The extensional viscosity was measured with an ARES rheometer at 110°C with the application of a prestretching rate of 0.01 s^{-1} and an extensional rate of 0.1 s^{-1} with an extensional viscosity fixture accessory. The dimensions of the specimens were 10 × 18 × 1 mm^3.

Differential scanning calorimetry (DSC) tests were done in a Pyris 6 DSC instrument under the following conditions: heating from 30 to 200°C at 10°C/min and cooling from 200 to 40°C at 10°C/min. The weight of the samples was around 5–6 mg.

RESULTS AND DISCUSSION

Morphology

From the elemental analysis, the actual contents of MB and SA in the NCPs were determined, as shown in Table II. In all cases, the amounts of MB and SA adsorbed were lower than the nominal amount; this was consistent with results obtained by other authors.[22]

Diffraction curves of the NC and the synthesized nanopigments are shown in Figure 1. As it is known,[15–17,20] the position of the diffraction peak was displaced toward lower angles when the percentage of MB exchanged in the NC increased as a consequence of the increase in the interlayer distance in the NC. Exceptionally, the position of the diffraction peak of the pigment exchanged at 20% with MB [NCP(20/0)] was lower than the one of the pigment exchanged at 100% [NCP(100/0)]; this indicated that there was greater interlamellar distance in NCP(20/0) than in NCP(100/0). According to other authors,[16] this may have been due to the high hydration of sodium, which could make the basal spacing higher than when there was more sodium replaced by the surfactant. Furthermore, we observed that the nanopigment exchanged with MB and SA [NCP(20/80)] presented an interlayer distance greater than that of the nanopigment exchanged 100% with MB [NCP(100/0)]. This implied that the presence of the SA enlarged the interlayer distance of the NC.

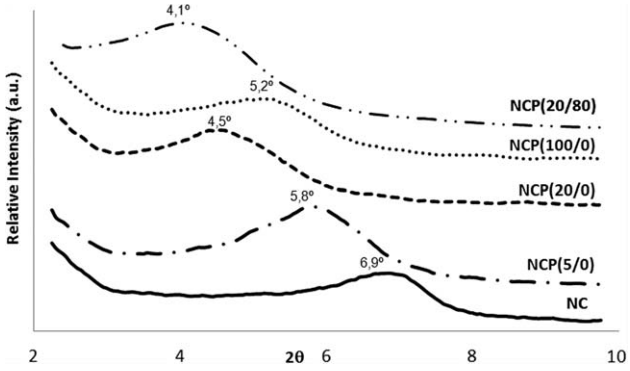

Figure 1. Diffraction curves of the nanopigments.

Figure 2 shows the diffraction curves for the EVA samples with nanopigments [EV–NCP(*X*/*Y*)] and with unmodified NC and MB [EV–NC-1–MB set]. In general, when an NC is incorporated into a polymeric matrix, there is a displacement of the diffraction peak of the clay toward lower 2θ angles because of

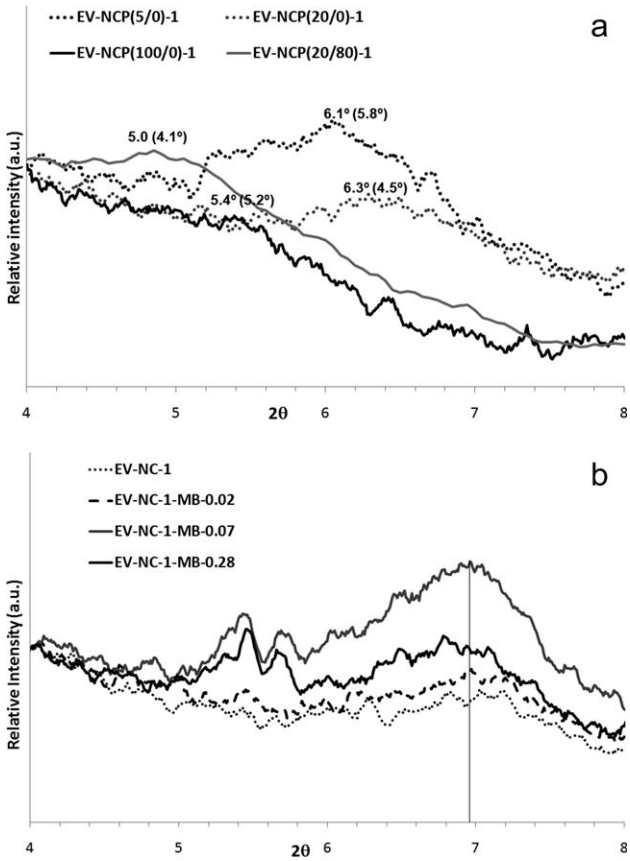

Figure 2. Diffraction curves of the sets of samples with (a) nanopigments EV–NCP(*X*/*Y*) and (b) unmodified NC and MB and EV–NC-1–MB.

Applied Polymer SCIENCE

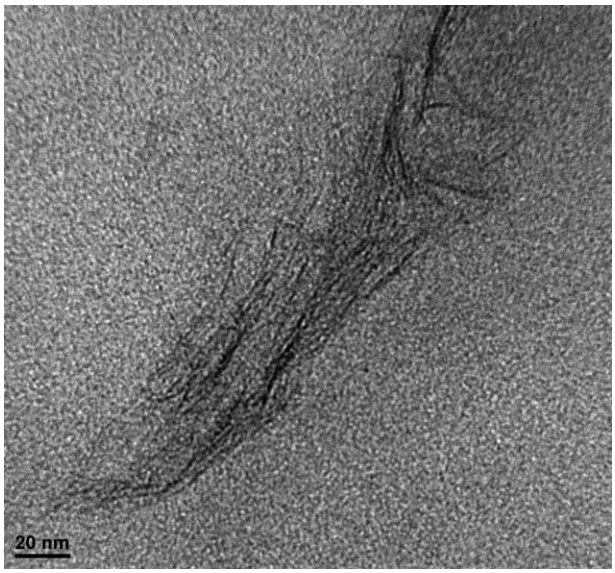

Figure 3. TEM image of the EV–NPC(20/80)-0.1 sample.

the increase in the interlayer distance in the NC. The peak broadens, which indicates that there is an increase in the disorder of the clay layers and a better dispersion. When the diffraction peak disappears, it is accepted that the clay layers are completely exfoliated.[6,8,13,23] Peak broadening was largely observed in the EVA composites [EV–NCP(*X*/*Y*) set] obtained with nanopigments, as shown in Figure 2(a). In this figure, the position of the diffraction peak and the position of the peak corresponding to the NCPs (between the brackets) are shown. In contrast to the results of other authors, when the position of the diffraction peak in each nanopigment to the position in the corresponding composite were compared, we observed that the peaks were displaced toward higher angles; this implied a reduction in the interlayer distance of the NCPs. Marini et al.[10] observed a similar behavior in EVA/organoclay composites. According to these authors, this phenomenon was caused by the removal of the surfactant from the modified clay due to the high shear stress during the processing of the samples. The composites containing the nanopigments NCP(20/0) and NCP(20/80) suffered a major displacement of the diffraction peak compared to those of the others. As mentioned previously, at relatively low exchange levels, the high hydration of sodium may have provoked a higher interlayer distance than expected. The loss of water during processing gave an extra peak displacement in these nanocomposites. The TEM images supported the fact that the morphological structure of the EVA/NCP composites was intercalated and partially exfoliated. Nevertheless, the composites containing the NC with the higher amount of surfactant [NCP(100/0) and NCP(20/80)] presented a high interlayer distance and broad peaks in XRD, and these samples also showed a more disordered structure, as shown in Figure 3, for the EVA–NCP(20/80)-0.1 composite.

In the EV–NC-1–MB set [Figure 2(b)], the diffraction peak remained in the same position as in the NC, about 6.9°; this was equivalent to an interlayer distance of 1.28 nm. This also indicated that the morphological structure of the EVA/NC/MB mixtures was intercalated with some clay clusters. Other authors obtained similar results in samples of EVA and unmodified NCs.[8,10] In addition, the diffraction peaks that corresponded to the MB, between 5.5 and 6°, were also identified in the samples with higher amounts of MB (EV–NC-1–MB-0.07 and EV–NC-1–MB-0.28). It is worth mentioning that even though that these samples contained the same amount of NC (1 phr), the height of the diffraction peak was higher as the amount of MB increased. The increase in the peak height indicated that the NC was more poorly dispersed in the EVA matrix as a consequence of the presence of MB.

Color Performance

Figure 4 shows the color performance parameters (the hiding power and coloring power) versus the content of MB for the EV–MB, EV–NC-1–MB and EV–NCP(*X*/*Y*) sets. As expected, the hiding power and coloring power increased when the content of MB in the sample increased. When NC was used (set EV–NC-1–MB versus set EV–MB) both parameters improve. The increase in these parameters, hiding power and coloring power, in the set of samples containing synthesized nanopigment [EV–NCP(*X*/*Y*)] was outstanding. It is worth pointing out that the content of dye in the sets shown in Figure 4 was the same. Therefore, the fact that the MB was supported in the NC, forming the nanopigment, remarkably boosted the color properties of the colorant. As was explained in a previous work,[20] the

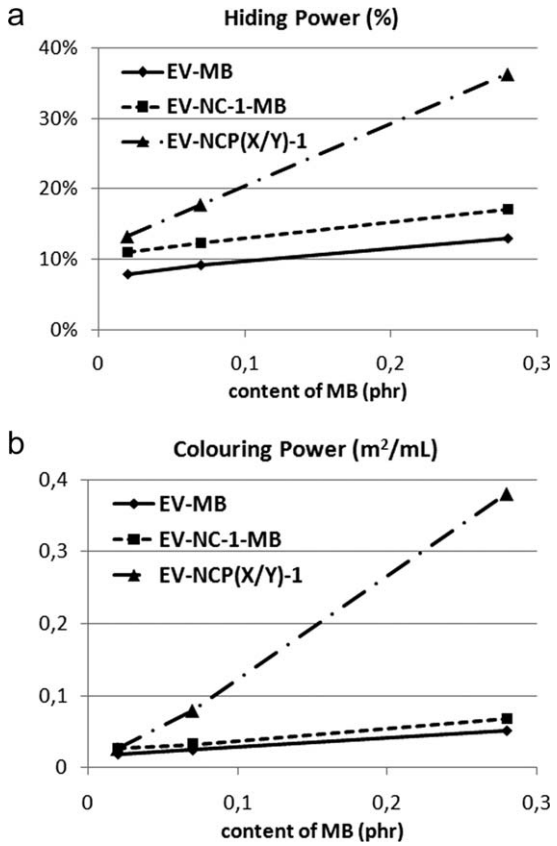

Figure 4. (a) Hiding power and (b) coloring power of the EV–MB, EV–NC-1–MB, and EV–NCP(*X*/*Y*) sets as a function of the MB content.

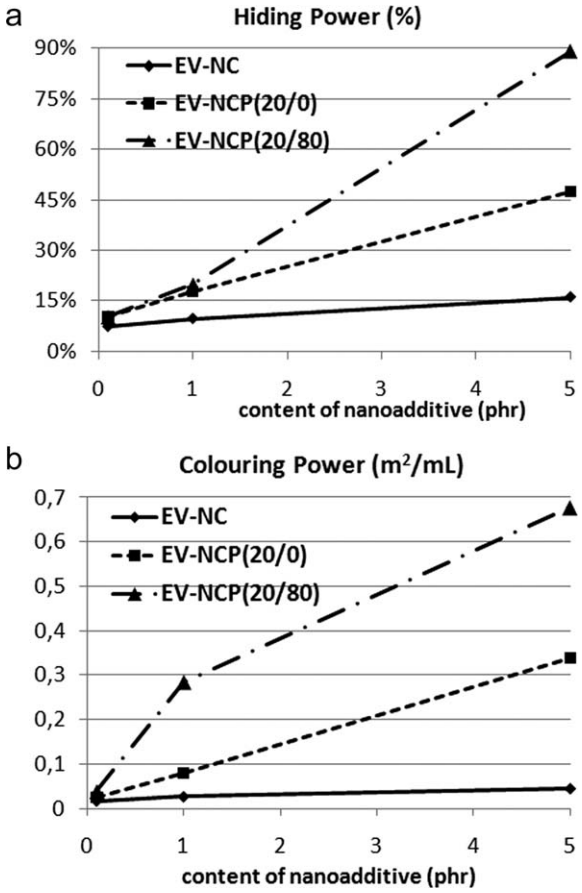

Figure 5. (a) Hiding power and (b) coloring power of the EV–NC, EV–NCP(20/0), and EV–NCP(20/80) sets as a function of NC or nanopigment content.

improvement in the color properties could have been due to the fact that when the MB was attached to the clay, the formation of aggregates was suppressed; thus, the dye interacted more effectively with the light, and this resulted in highly intense colors.

Figure 5 shows the color performance parameters (the hiding power and coloring power) versus the content of nanoadditive in the EV–NC, EV–NCP(20/0), and EV–NCP(20/80) sets. The NC itself provided opacity and a yellowish shade to the samples of the EV–NC set. The sets with nanopigments [NCP(20/0) and NCP(20/80)] also presented an increasing tendency when the content of additive was increased. However, at the same concentration, the samples with NCP(20/80) exhibited a higher color performance than the samples with NCP(20/0). This could be explained as a consequence of a better level of exfoliation and dispersion of the nanopigments NCP(20/80) than NCP(20/0). Therefore, the presence of the SA boosted the colorimetric properties of the nanopigments.

Migration

There was no bleeding of the organic dye out of the EVA matrix in any of the samples prepared with the NCPs, as shown in Figure 6, which shows the samples with higher content of NCPs.

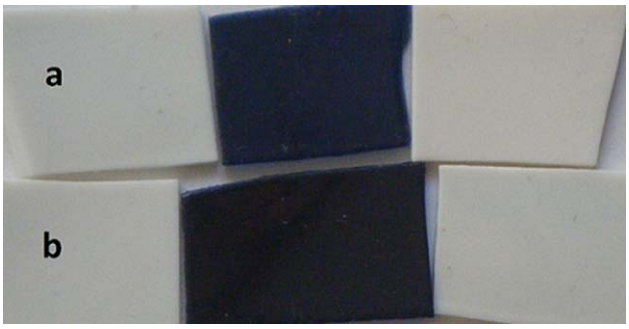

Figure 6. Bleeding test images for the (a) EV–NCP(20/0)-5 and (b) EV–NCP(20/80)-5 samples. [Color figure can be viewed in the online issue, which is available at wileyonlinelibrary.com.]

Nevertheless, migration was observed in the samples where the dye was not supported by NC (EV–MB).

DSC

The crystallization temperatures (T_c's; °C) and crystallization enthalpies (ΔH_c's; J/g) are shown in Table III. The T_c's of the mixtures were slightly higher than that of EVA; this indicated that the crystals were smaller in the composites. In general, the crystallinity of the mixtures was lower than that of EVA. Even though there was no clear trend of these parameters with the amount of nanoadditive, we observed that the value of ΔH_c linearly decreased when the content of MB in the EVA/NCP composites was increased. These results were in accordance with the observations of Chaudhary et al.,[8] who suggested that exfoliated clay platelets could form a network structure, reducing the mobility of the amorphous phase in the molten state and then suppressing the crystallinity. As was observed through XRD and

Table III. T_c (°C) and ΔH_c (J/g) Values of the Samples

Sample	T_c (°C)	ΔH_c (J/g)
EVA	69.3	35.6
EV-NC-0.1	70.5	37.0
EV-NC-1	70.7	40.3
EV-NC-5	70.1	29.1
EV-MB-0.02	69.9	29.6
EV-MB-0.07	70.1	23.1
EV-MB-0.28	70.2	28.4
EV-NC-1-MB-0.02	69.8	32.1
EV-NC-1-MB-0.07	70.3	35.5
EV-NC-1-MB-0.28	70.3	31.4
EV-NCP(5/0)-1	70.3	32.7
EV-NCP(20/0)-1	70.9	29.3
EV-NCP(100/0)-1	70.1	26.3
EV-NCP(20/0)-0.1	70.5	33.2
EV-NCP(20/0)-1	70.9	29.3
EV-NCP(20/0)-5	69.9	17.8
EV-NCP(20/80)-0.1	70.5	26.8
EV-NCP(20/80)-1	70.3	28.3
EV-NCP(20/80)-5	70.2	36.0

Applied Polymer SCIENCE

Table IV. E (MPa) and E_{ab} (J) Values

Sample	E (MPa)	E_{ab} (J)
EVA	17.0±0.7	20.2±1.7
EV–NC-0.1	18.3± 0.7	20.9± 1.1
EV–NC-1	17.5± 0.5	19.3± 1.3
EV–NC-5	19.2± 0.7	16.3± 0.4
EV–MB-0.02	15.6± 0.5	16.8± 0.4
EV–MB-0.07	16.0± 0.4	18.4± 1.5
EV–MB-0.28	18.0± 0.9	13.3± 1.2
EV–NC-1	17.5± 0.5	19.3± 1.3
EV–NC-1–MB-0.02	16.8± 0.3	16.1± 2.6
EV–NC-1–MB-0.07	17.5± 0.8	18.8± 1.7
EV–NC-1–MB-0.28	17.5± 0.5	15.8± 2.7
EV–NCP(5/0)-1	17.6± 0.5	16.6± 1.8
EV–NCP(20/0)-1	17.7± 0.5	19.0± 1.5
EV–NCP(100/0)-1	18.0± 0.5	16.2± 1.4
EV–NCP(20/0)-0.1	17.1± 0.6	17.4± 1.9
EV–NCP(20/0)-1	17.7± 0.5	19.0± 1.5
EV–NPC(20/0)-5	19.5± 0.5	18.2± 1.0
EV–NCP(20/80)-0.1	17.8± 0.6	19.6± 1.2
EV–NCP(20/80)-1	17.1± 0.4	18.2± 0.8
EV–NCP(20/80)-5	19.8± 0.5	18.1± 2.2

Table V. $T_{max,1}$ (°C) and $T_{max,2}$ (°C) of the Samples

Sample	$T_{max,1}$ (°C)	$T_{max,2}$ (°C)
EVA	357.0	479.9
EV–MB-0.02	349.2	459.2
EV–MB-0.07	345.5	453.4
EV–MB-0.28	342.7	451.9
EV–NC-1–MB-0.02	348.0	463.4
EV–NC-1–MB-0.07	353.0	465.0
EV–NC-1–MB-0.28	345.4	455.4
EV–NCP(5/0)-1	378.9	486.7
EV–NCP(20/0)-1	361.0	478.1
EV–NCP(100/0)-1	365.9	472.2
EV–NC-0.1	358.5	478.7
EV–NC-1	355.4	471.0
EV–NC-5	355.9	466.5
EV–NCP(20/0)-0.1	356.9	475.0
EV–NCP(20/0)-1	361.0	478.1
EV–NCP(20/0)-5	359.6	476.0
EV–NCP(20/80)-0.1	350.4	475.9
EV–NCP(20/80)-1	351.6	474.1
EV–NCP(20/80)-5	351.6	476.1

TEM, the exfoliation and dispersion of the NC increased in the EV–NCP(X/Y) set with the surfactant content, and consequently, the crystallization was reduced.

Mechanical Strength

Traction test results are shown in Table IV. In general, the Young's modulus (E) values were quite similar, and only the samples with a higher concentration of NC or NCP (5 phr) presented a higher value. Several authors have observed an increase in E values in EVA nanocomposites with increasing concentration of NC,[8,23] as was observed in this study. We believe that the increase in E was due to an increase in the rigidity provided by the NC, and as the specific surface area was increased, the stress was better transferred through the matrix to the NC. That would be the reason why the samples with a higher amount of nanoadditive [EV–NC-5, EV–NCP(20/0)-5, and EV–NCP(20/80)-5)] showed an increase in E.

On the other hand, almost all of the samples presented a lower energy absorbed at break (E_{ab}) than the EVA. The presence of NC tactoids reduced the capacity of the material to absorb energy as a consequence of a reduction in the mobility of the polymer chain.[8,23] Consequently, E_{ab} decreased when the amount of nanoadditive increased. However, the reduction of E_{ab} was less noticeable in samples with nanopigments than in samples with unmodified clay.

Thermal Stability

In the thermal degradation of EVA, two processes could be identified. There was a first loss of mass that corresponded to the removal of the acetate groups. This started at about 300°C and reached the maximum degradation rate at approximately 350°C. In the second step, the remaining hydrocarbon chains were degraded, and the maximum degradation rate reached about 480°C.[24]

Table V shows the temperatures at the maximum degradation rate in both decomposition processes ($T_{max,1}$ and $T_{max,2}$) for the samples. In all cases, we observed that the presence of MB (set EV–MB) reduced the thermal stability of the EVA as $T_{max,1}$ and $T_{max,2}$ were reduced. When 1 phr NC was added to the EV–NC-1–MB samples, the thermal stability increased with respect to the EV–MB samples. However, when the nanopigment was incorporated [set EV–NCP(X/Y)], the thermal stability of the samples improved, even more than for the EVA sample. On the other hand, when the content of MB in the nanopigment increased, the thermal stability of the system was reduced. This could be seen in the decrease of $T_{max,1}$ and $T_{max,2}$ (Table V).

On the other hand, samples of the NCP(20/0) and NCP(20/80) sets did not show significant modification in the thermal stability, regardless of the nanoadditive load. However, in the EV–NC set, the thermal stability of the samples was reduced when the load of NC was increased. In a previous study,[21] it was observed that the thermal stability of the first step of degradation of EVA was reduced with the content of organomodified clay, whereas the stability in the second step of degradation was increased; this was in accordance with the results obtained by other authors.[9,12,25] The reduction of the thermal stability in the first step of the decomposition process of EVA was justified in part by the fact that the acidic sites in the clay catalyzed the loss of acetic acid in EVA and because of the degradation of the surfactant itself. The surfactant used in this study (MB) was much more thermally stable than the ammonium salts that were used in the previously mentioned works. This would help to explain

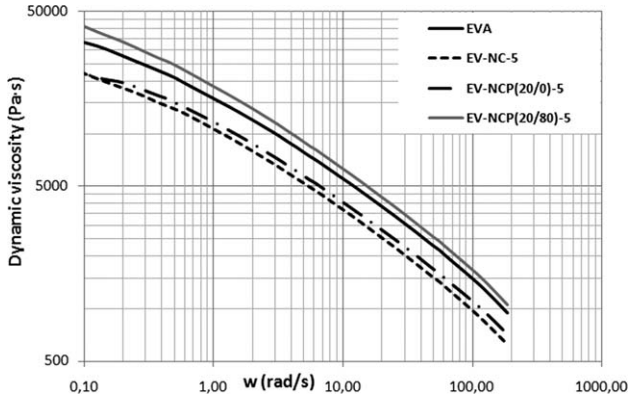

Figure 7. Dynamic viscosities of the EV–NC-5, EV–NCP(20/0)-5, and EV–NCP(20/80)-5 samples.

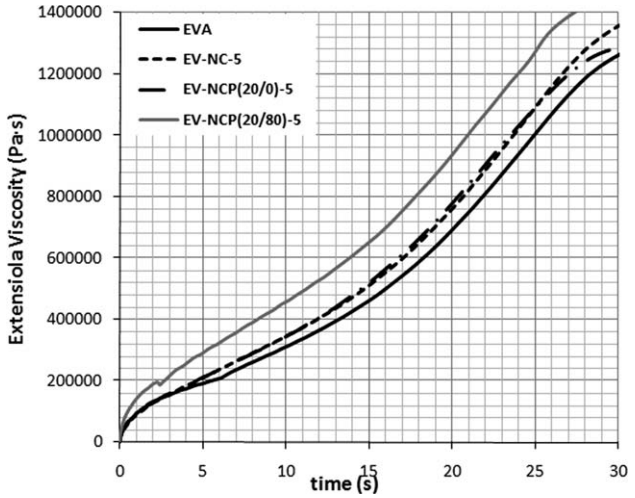

Figure 8. Extensional viscosities of the EV–NC-5, EV–NCP(20/0)-5, and EV–NCP(20/80)-5 samples.

that the thermal stability of the EV–NCP(20/0) and EV–NCP(20/80) sets did not change significantly during the first decomposition step in these series. On the other hand, the increase in the thermal stability in the second step was explained in those articles as a consequence of the barrier properties of the NC, which depend on the level of exfoliation. When the clay layers were exfoliated, they may have reduced the volatilization of the degradation products, and then, the thermal stability increased. That would also help to explain that the samples of the EV–NCP(20/0) and EV–NCP(20/80) sets, which were better dispersed than the samples of the EV–NC set, had a similar thermal stability as EVA and a better thermal stability than the samples with unmodified clay (EV–NC).

Dynamic and Extensional Viscosities

The dynamic and extensional viscosities of the EV–MB, EV–NC-1–MB, and EV–NCP(*X*/*Y*) sets did not show any significant difference compared to EVA. Figure 7 shows the dynamic behavior of EVA and the corresponding mixtures with 5 phr NC, NCP(20/0) and NCP(20/80). Samples with NC and NCP(20/0) had lower dynamic viscosities than EVA. Several authors have reported a similar behavior in EVA–NC composites.[4,6,10,25,26] According to these authors, clay layers are able to align and reorient in the flow direction, acting somehow as lubricants and leading to a decrease in the viscosity of the system. The behavior of the sample with NCP(20/80) was different. The presence of the SA led to a better exfoliation and dispersion of the clay platelets and thus to an increase in the viscosity. As a result, the interactions between polymer chains and clay layers may have increased, and this would have caused a higher resistance to the deformations and thus a higher viscosity. This was in accordance with the results of other authors.[4,5,10]

With regard to the extensional viscosity, the more concentrated samples, EV–NC-5, EV–NCP(20/0)-5, and EV–NCP(20/80)-5, had higher extensional viscosities than EVA (Figure 8). In this case, the three samples exhibited an increase in the extensional viscosity, but it was more pronounced in the sample with NCP(20/80) than in the others. This could be explained because of its more exfoliated and dispersed structure. When the clay layers were exfoliated, there were more polymer–clay layer interactions; these increased the opposition to the extensional flow and deformation. Prasad et al.[26] obtained similar results in EVA–organoclay nanocomposites. At a high loading, the extensional viscosity in the linear region increased slightly compared to the unfilled polymer. This behavior was explained as a consequence of an increase in the interactions among clay layers in the three dimensions at a high clay loading. Furthermore, several authors have described an increase in the extensional viscosity of EVA nanocomposites when the interlayer distance in the clay sheets is enlarged,[5] as was observed here for the EV–NCP(20/80)-5 composite.

CONCLUSIONS

NCPs used with a linear low-density PE in a previous study were applied to EVA. The EVA/NCP composites' hiding and coloring powers increased fairly with respect to those of the EVA/dye and EVA/NC/MB samples. This was probably because the support of MB in the NC prevented the aggregation of dye, and it could develop more color. Moreover, a series of NCPs, including two surfactants, MB and an SA, was successfully synthesized. The presence of the SA in the nanopigment boosted the color performance remarkably compared to that of the composites of nanopigments without salt. The SA improved the exfoliation and dispersion of the NCPs in EVA and, therefore, improved the color performance. Furthermore, there was no MB bleeding out of the polymeric matrix in the samples prepared with nanopigments.

The prepared EVA/NCP composites presented an intercalated and partially exfoliated structure. The presence of NC, MB, or both without previous exchange (i.e., not forming a NCP but a physical mixture) reduced the thermal stability of the EVA samples. In contrast, when the NCPs were used, the stability was slightly improved. *E* increased in the more exfoliated and NCP concentrated samples. With respect to the dynamic viscosity, NC and NCP(20/0) acted as lubricants, decreasing the dynamic viscosity, but in the sample with NCP(20/80), which was the more exfoliated one, the dynamic viscosity increased because the polymer–clay layer interactions made the system deformation difficult. All of samples studied and especially NCP(20/80)

presented a higher extensional viscosity as the interlayer distance increased.

ACKNOWLEDGMENTS

The authors thank The Netherlands Organisation for Applied Scientific Research, Eindhoven, especially Hartmut Fischer and Lawrence Batenburg, for allowing them to reproduce the synthesis of Planocolors and for their technical support and knowledge. One of the authors (V.M.R.) thanks the Conselleria d'Empresa, Universitat i Ciència, for a Ph.D. grant (contract grant number BFPI/2007/038) that she received.

REFERENCES

1. Pavlidou, S.; Papaspyrides, C. D. *Prog. Polym. Sci.* **2008**, *33*, 1119.
2. Zeng, Q. H.; Yu, A. B.; Lu, G. Q. M.; Paul, D. R. *J. Nanosci. Nanotechnol.* **2005**, *5*, 1574.
3. Livi, S.; Duchet-Rumeau, J.; Pham, T. N.; Gérard, J. F. *J. Colloid Interface Sci.* **2010**, *349*, 424.
4. Pasanovic-Zujo, V.; Gupta, R. K.; Bhattacharya, S. N. *Rheol. Acta* **2004**, *43*, 99.
5. La Mantia, F. P.; Dintcheva, N. T. *Polym. Test.* **2006**, *25*, 701.
6. Gianelli, W.; Camino, G.; Dintcheva, N. T.; Verso, S. L.; Mantia, F. P. L. *Macromol. Mater. Eng.* **2004**, *289*, 238.
7. Zhang, W.; Chen, D.; Zhao, Q.; Fang, Y. *Polymer* **2003**, *44*, 7953.
8. Chaudhary, D. S.; Prasad, R.; Gupta, R. K.; Bhattacharya, S. N. *Thermochim. Acta* **2005**, *433*, 187.
9. Valera-Zaragoza, M.; Ramírez-Vargas, E.; Medellín-Rodriguez, F. J.; Huerta-Martínez, B. M. *Polym. Degrad. Stab.* **2006**, *91*, 1319.
10. Marini, J.; Branciforti, M. C.; Lotti, C. *Polym. Adv. Technol.* **2010**, *21*, 408.
11. Jeon, C. H.; Ryu, S. H.; Chang, Y.-W. *Polym. Int.* **2003**, *52*, 153.
12. Wilson, R.; Plivelic, T. S.; Aprem, A. S.; Ranganathaiagh, C.; Kumar, S. A.; Thomas, S. *J. Appl. Polym. Sci.* **2012**, *123*, 3806.
13. Gupta, R. K.; Pasanovic-Zujo, V.; Bhattacharya, S. N. *J. Non-Newton. Fluids* **2005**, *128*, 116.
14. Stoeffler, K.; Lafleur, P. G.; Denault, J. *Polym. Eng. Sci.* **2008**, *48*, 1449.
15. He, H.; Ma, Y.; Zhu, J.; Yuan, P.; Qiung, Y. *Appl. Clay Sci.* **2010**, *48*, 67.
16. Xi, Y.; Frost, R. L.; He, H. *J. Colloid Interface Sci.* **2007**, *305*, 150.
17. Jincheng, W.; Xiaoyu, Z.; Wenli, H.; Nan, X.; Xingchen, P. *Powder Technol.* **2010**, *221*, 80.
18. Fischer, H.; Batenburg, L. F. Pat. WO0104216, The Netherlands (**2001**).
19. Marchante, V.; Martinez-Verdu, F.; Beltran, M.; Marcilla, A. *Pigment Resin Technol.* **2012**, *41*, 5.
20. Marchante, V.; Marcilla, A.; Benavente, V.; Martínez-Verdú, F. M.; Beltrán, M. I. *J. Appl. Polym. Sci.* [accessed on Feb 1, 2013]. DOI: 10.1002/app.38903. Published Online:Feb 1, **2013**. http://onlinelibrary.wiley.com/doi/10.1002/app.38903/abstract.
21. Beltrán, M. I.; Benavente, V.; Marchante, V.; Marcilla, A. *Appl. Clay Sci.*, accepted.
22. Jankovic, L.; Madejova, J.; Komadel, P.; Jochec-Moskova, D.; Chodak. I. *Appl. Clay Sci.* **2011**, *51*, 438.
23. Ugel, E. *Soft Nanosci. Lett.* **2011**, *1*, 105.
24. Marcilla, A.; Beltrán, M. *Polym. Degrad. Stab.* **1995**, *50*, 117.
25. Lee, H. M.; Park, B. J.; Choi, H. J.; Gupta, R. K.; Bhattacharya, S. *J. Macromol. Sci. Part B* **2007**, *46*, 261.
26. Prasad, R.; Pasanovic-Zujo, V.; Gupta, R. K.; Cser, F.; Bhattacharya, S. N. *Polym. Eng. Sci.* **2004**, *44*, 1220.